Front. Optoelectron. 2019, 12(4): 397–404
https://doi.org/10.1007/s12200-019-0866-9

RESEARCH ARTICLE

Airy-like field under high numerical aperture optical system

Yong LIU[1,2], Zhifeng ZHANG[2,3], Cuifang KUANG (✉)[2,4]

1 College of Electronics and Information Engineering, Shanghai University of Electrical Power, Shanghai 200090, China
2 State Key Laboratory of Modern Optical Instrumentation, College of Optical Science and Engineering, Zhejiang University, Hangzhou 310027, China
3 School of Physics and Electronic Engineering, Zhengzhou University of Light Industry, Zhengzhou 450002, China
4 Collaborative Innovation Center of Extreme Optics, Shanxi University, Taiyuan 030006, China

Abstract The tightly focused field of an incident light beam through cubic phase modulation has been investigated by vectorial diffraction theory. For different modulation index of cubic phase and polarization states of the incident light, the focused fields have been presented. The results show that the Airy-like field can be produced by cubic phase modulation under high numerical aperture (NA) optical system. Intensity pattern and length of the main lobe are depended on modulation index for the spatial uniform polarization, and the Airy-like field is affected by polarization state for the spatial nonuniform polarization. It is helpful to structure new optical fields in optical manipulation, optical imaging, and surface plasma controlling.

Keywords diffraction, cubic phase, optical field, Airy beam

1 Introduction

In 1979, Berry and Balazs [1] first demonstrated that a nonspreading Airy wave packet solution is satisfied to the potential-free Schrodinger equation in theory. Then, based on the Fourier transform, the finite-energy Airy wave packet is a Gauss beam modulated with cubic phase. Siviloglou et al. [2] reported the first observation of Airy beam, which can exhibit unusual optical features such as the nondiffraction propagation and free acceleration over a long distance. Justly due to the distinctive properties of nondiffraction, self-healing, transverse acceleration and autofocusing, Airy beams have exhibited tremendous application potentials in these fields [3–13], for example, optical microscopy, spatiotemporal Airy light bullets, optical micromanipulation of particles, and surface plasma control.

For the generation of Airy beam, the general method is cubic phase modulation of a Gauss beam in optical Fourier transform system, due to the relation between Gauss function with cubic phase and Airy function. At present, the cubic phase modulation can be implemented by spatial light modulation, quadratic nonlinear photonic crystal, polymer-dispersed liquid crystals (PDLC) with a binary phase pattern, liquid crystals with a binary phase pattern electrode, nanograting and continuous phase plate [14–20]. Meanwhile, based on the approximate expression of Airy function, 3/2 phase modulation could be exploited to directly generate Airy beam and the optical Fourier transform system was not necessary [21]. By the geometrical properties of paraxial or non-paraxial optical caustics and the Legendre transform, direct spatial phase encoding and imaging could generate arbitrary convex accelerating optical beams [22]. When cubic phase collaborated with one-dimension (1D) binary function, the main lobe of super-Airy beam could present smaller size and higher intensity than the main lobe of Airy beam [23]. Obviously, these aforementioned optical systems and methods based on Fourier transformation or Fresnel diffraction did not involve the vectorial character of optical diffraction. To comprehensively analyze Airy beam, many nonparaxial and vectorial methods [24–27] were presented, and the new family of Airy beam can be generated.

The high numerical aperture (NA) optical system can also be analyzed by the vectorial diffraction theory, wherein a small focus and short focal depth appears. Furthermore, the focused field often relates to the polarization state of the incident light beam. If special optical fields can be produced by phase or polarization modulation, where the focus size lies on high NA and the

Received November 22, 2018; accepted December 17, 2018

E-mail: cfkuang@zju.edu.cn

focal depth has long length, this will make them find more applications. Considering the nondiffraction character of Airy beam, the wavefront coded by cubic phase mask or squared cubic phase mask was directly exploited to engineer point spread functions in optical imaging system [28,29], but the tightly focused field generated directly by cubic phase modulation had not been fully investigated. Therefore, under the high NA optical system, it is very necessary to exploit these important physics parameters to structure the new focused field, such as phase modulation strength of cubic phase and polarization state of the incident light beam. In this paper, we investigated the tightly focused field generated by cubic phase modulation. Through the vectorial diffraction theory, the optical intensity distribution near the focus was presented. By the numerical simulation, different focused optical fields were generated and analyzed. Finally, the relations between Airy-like field, modulation index of cubic phase and polarization state of the incident light were presented.

2 Theory

In the proposed optical system, the parallel light beam is collimated and conveyed through a cubic phase plate, then focused by a high-NA objective lens. The tightly focused field can be presented by the vectorial diffraction theory [30]. Here, the cubic phase distribution $P(x, y)$ in the exit aperture of objective lens can be expressed as

$$P(x,y) = \exp\{\mathrm{i}\alpha[(x+y)^3 + (x-y)^3]\}, \quad (1)$$

where α is the modulation index. x and y are the Cartesian coordinates in the exit aperture plane. For Airy beam, the direction of transverse acceleration is depended on the sign of α.

When the high-NA objective lens without aberration is satisfied to Abbe's sine condition, the tightly focused field of incident beam with different amplitude, phase and polarization can be expressed as

$$\vec{E}(r_2,\varphi_2,z_2) = \mathrm{i}C\int_0^{\beta}\int_0^{2\pi}\sqrt{\cos\theta}E_0(\theta,\varphi)A(\theta,\varphi)P(\theta,\varphi)\begin{bmatrix} px \\ py \\ pz \end{bmatrix} \mathrm{e}^{\mathrm{i}kn(z_2\cos\theta + r_2\sin\theta\cos(\varphi-\varphi_2))}\sin\theta\mathrm{d}\theta\mathrm{d}\varphi, \quad (2)$$

where $\vec{E}(r_2,\varphi_2,z_2)$ is the electric field at the point (r_2,φ_2,z_2) near the focus, and C is the normalized constant. Integral upper limit β is equal to arcsin(NA/ n). Here, NA is the numerical aperture of the objective, and n is the refractive index of the focal region. $\sqrt{\cos\theta}$ is the apodization factor, and $E_0(\theta, \varphi)$ is the amplitude distribution of incident light beam. $P(\theta, \varphi)$ is the expression of Eq. (1) under the cylindrical coordinates, based on $x = f\sin\theta\cos\varphi$ and $y = f\sin\theta\sin\varphi$. f is the focal length of the high-NA objective lens. k is the wave number of the focal region and equals $2\pi n/\lambda$. $A(\theta,\varphi)$ is a 3×3 matrix related with the structure of the objective lens. For the aplanatic lens, $A(\theta,\varphi)$ can be expressed as

$$A(\theta,\varphi) = \begin{bmatrix} 1+(\cos\theta-1)\cos^2\varphi & (\cos\theta-1)\cos\varphi\sin\varphi & -\sin\theta\cos\varphi \\ (\cos\theta-1)\cos\varphi\sin\varphi & 1+(\cos\theta-1)\sin^2\varphi & -\sin\theta\sin\varphi \\ \sin\theta\cos\varphi & \sin\theta\sin\varphi & \cos\theta \end{bmatrix}. \quad (3)$$

The matrix unit vector, [px; py; pz], which depends on the polarization states of incident light beam, can be expressed as

$$\begin{bmatrix} px \\ py \\ pz \end{bmatrix} = \begin{bmatrix} 1 \\ 0 \\ 0 \end{bmatrix} \quad \text{Linear polarization along } x-\text{axis}, \quad (4\text{–}1)$$

$$\begin{bmatrix} px \\ py \\ pz \end{bmatrix} = \frac{1}{\sqrt{2}}\begin{bmatrix} 1 \\ i \\ 0 \end{bmatrix} \quad \text{Right circular polarization}, \quad (4\text{–}2)$$

$$\begin{bmatrix} px \\ py \\ pz \end{bmatrix} = \begin{bmatrix} \cos\theta \\ \sin\theta \\ 0 \end{bmatrix} \quad \text{Radial polarization}, \quad (4\text{–}3)$$

$$\begin{bmatrix} px \\ py \\ pz \end{bmatrix} = \begin{bmatrix} -\sin\theta \\ \cos\theta \\ 0 \end{bmatrix} \quad \text{Azimuthalpolarization}. \quad (4\text{–}4)$$

Therefore, the electric intensity distributions of tightly focused field generated by cubic phase modulation are given by $I = |E_{r2}|^2 + |E_{\varphi 2}|^2 + |E_{z2}|^2$.

3 Simulation and discussion

To investigate the tightly focused optical field generated in the proposed optical system, we suppose that the amplitude distribution of incident light beam $E_0(\theta, \varphi)$ is Gauss function, and equals to $\exp(-\eta^2\sin^2\theta/\sin^2\beta)$. Here, η is the ratio of the pupil radius to the beam waist, and assumed to be 1/2 as an example in this case. When the incident light beam with wavelength of 500 nm is circular polarization,

the focused optical fields through a high-NA oil-immersion objective of NA = 1.4 and n = 1.518 are simulated by Eq. (2), whose pupil radius is 10 mm.

Based on Eq. (1), the cubic phase masks with different modulation index α are shown in Fig. 1. The wrapped phase is from $-\pi$ to π. Obviously, there are two symmetry axes in the phase map. Here, the phase map is symmetric to the x-axis, but is antisymmetric to the y-axis, which determines the acceleration direction along the x-axis for Airy beam [23]. Considering the electric fields shown in Eq. (2), when the phase map, amplitude and polarization distribution are rotational symmetric, the focused fields of high NA optical system without aberration will also be rotational symmetric. Under the above assumed condition, this means that the focused fields modulated by the cubic phase maybe have transverse acceleration. Meanwhile, the central part looking like an "eye" in cubic phase has relatively slow phase modulation along the y-axis, but the outer part locating away from the "eye" has fast phase modulation. Therefore, modulation index can determine the weight between slow and fast phase part, then make the focused field take a change.

For illuminating the effect of cubic phase, the focused optical fields normalized by the intensity peak of the main lobe in the focal plane are presented in Fig. 2. When $\alpha = 0$, it is corresponding to the case without cubic phase modulation shown in Figs. 2(a)–2(c), the tightly focused fields are rotational symmetric at the transverse plane, but the intensity values and patterns will take a change with the increasing of z. Here, we define the nondiffraction length as the distance between the two transverse planes, where the intensity peak is equal to the 1/2 of intensity peak in the focal plane. Thus, the nondiffraction length is about λ for the case of $\alpha = 0$. For the case of cubic phase with $\alpha = 0.01$, the different focused fields are presented in Figs. 2(d)–2(i). Note that one main lobe with some minor lobes conveys most of light energy along several diffraction lengths, and all lobes hold on transverse acceleration along the x-axis, which is similar to the case of Airy beam. So, we define this focused field as Airy-like field. Considering the phase distribution in Fig. 1, the acceleration direction of the Airy-like field can be determined by the location of symmetry axis (x-axis) in cubic phase map. While the intensity patterns of main lobe along the acceleration trajectory take some change, the main lobe can carry certain light energy from $z = -6.8\lambda$ to 6.8λ. Compared with the case without cubic phase modulation, the nondiffraction length is enlarged about 14 times. Here, Figs. 2(b) and 2(e) depict the optical fields in the focal plane. Note that the position, shape and size of main lobe are changed by the cubic phase. Compared with the Gauss spot at the focal plane, the main lobe locates at $(-0.68\lambda, 0)$, takes on coma shape, and has a larger area. Due to the cubic phase part involving in coma aberration of the optical system, cubic phase modulation in our proposed system has the similar effect, which makes the main lobe take a change along the acceleration trajectory. This is corresponding to Figs. 2(d)–2(h). Especially, there are two areas near $z = -5\lambda$ and 5λ in Fig. 2 (d), in which the main lobe takes an obvious change and minor lobes become weaker. From the three-dimensional optical field shown in Fig. 2(i), note that the intensity pattern of the main lobe is transformed from triangle shape to oval shape, and the size of the main lobe is decreased. This case can be further proved in Figs. 2(g) and 2(h). Considering of Eq. (2), in high NA optical system, the tightly focused field is not perfect Fourier transform of Gauss beam with cubic phase. In theory, this induces the intensity patterns and acceleration trajectory of the main lobe in the focused field differ from the main lobe of Airy beam, but the Airy-like field simultaneously keeps some characteristics of Airy beam. Therefore, cubic phase modulation can produce Airy-like field in the high NA optical system.

To further investigate the effect of α, the normalized longitudinal and transverse optical fields are presented in Fig. 3. Note that the direction of transverse acceleration is not changing for different α, which once demonstrates the acceleration direction of Airy-like field is determined by the symmetry of cubic phase map. When α takes a smaller value, the nondiffraction length of Airy-like field decreases, these minor lobes become weaker, and the intensity patterns of the main lobe along the acceleration trajectory become more uniform. Obviously, compared with Figs. 3(b) and 3(c), Fig. 3(a) has no two areas, in which the intensity patterns of the main lobe will transform. If $\alpha \leqslant 0.0005$, cubic phase modulation almost takes no effect, thus the main lobe gradually becomes the Gaussian circular spot. However, with the increasing of

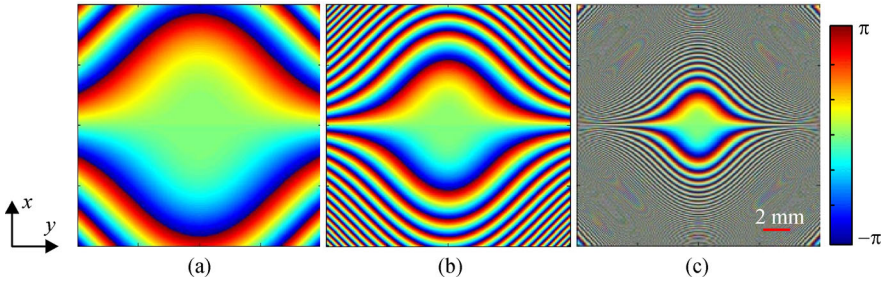

Fig. 1 Cubic phase masks with different modulation indexes. (a) $\alpha = 0.002$; (b) $\alpha = 0.01$; (c) $\alpha = 0.08$

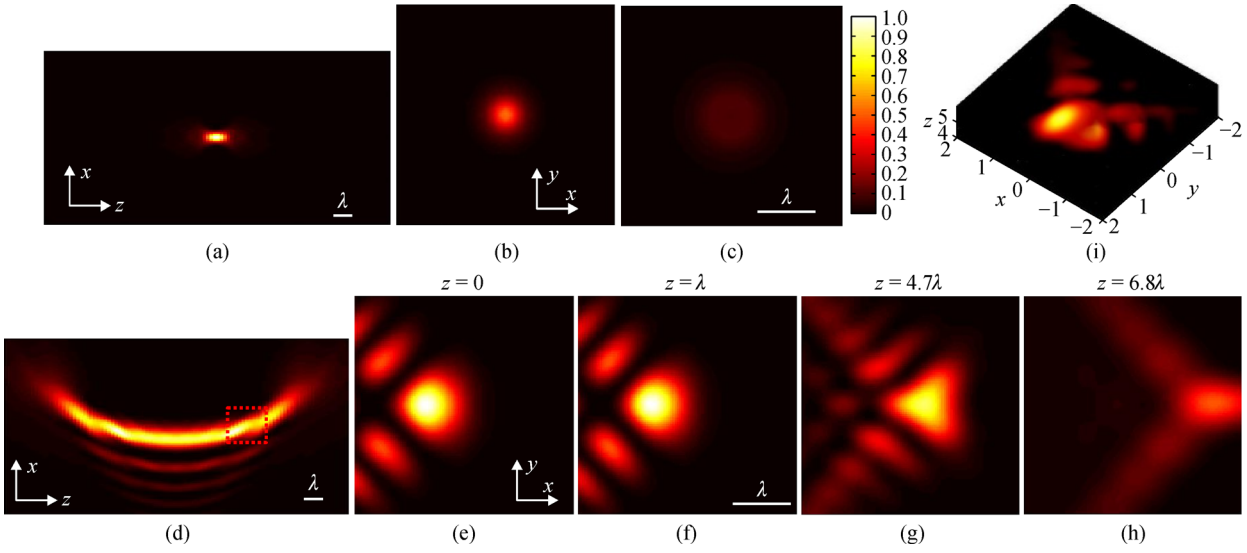

Fig. 2 Normalized optical fields modulated without and with cubic phase. When $\alpha = 0$, the longitudinal optical field through the focus is (a), the transverse optical fields are at (b) $z = 0$ and (c) $z = 0.5\lambda$. When $\alpha = 0.01$, the longitudinal optical field through the focus is (d), the transverse optical fields are at (e) $z = 0$, (f) $z = \lambda$, (g) $z = 4.7\lambda$, and (h) $z = 6.8\lambda$. Here, (i) is corresponding to the area shown by the dashed box in (d)

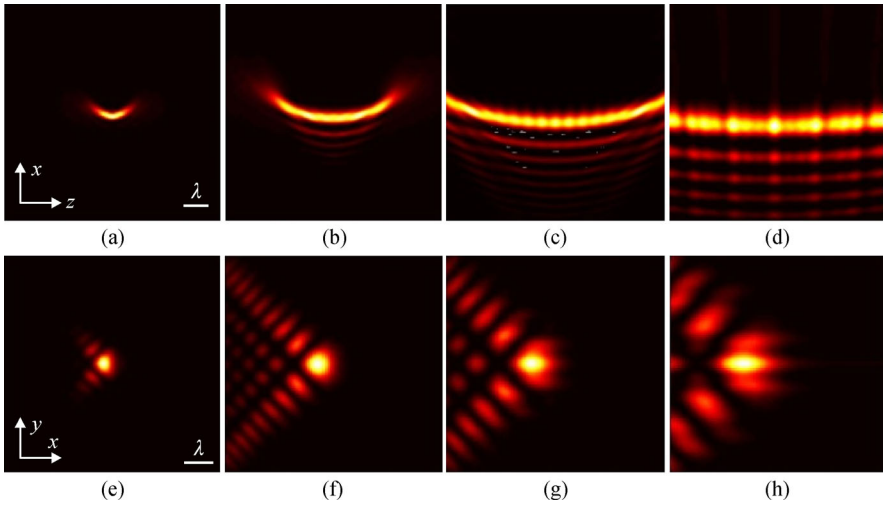

Fig. 3 Normalized optical fields modulated by different cubic phase. The longitudinal optical fields through the focus are (a)–(d) and the transverse optical fields in the focal plane are (e)–(h), for the case of $\alpha = 0.002$, 0.008, 0.02, and 0.06, respectively

modulation index, Figs. 3(c) and 3(d) show that the intensity patterns of the main lobe first take on pearl shape near the focus, then become pearl shape with different size. If $\alpha \geqslant 0.14$, the intensity patterns of main and minor lobes become optical speckles. Thus, when α is from 0.0005 to 0.14, Airy-like field can be produced in this case. Based on the optical fields shown in Figs. 3(a)–3(h), when α is 0.002, 0.008, 0.02, and 0.06, respectively, the location of main lobes in the focal plane is (–0.36λ, 0), (–0.6λ, 0), (–0.84λ, 0), and (–1.2λ, 0). Meanwhile, the nondiffraction lengths of Airy-like field are about 2.4λ, 11λ, 21λ, and 56λ. These results show that the increasing of modulation index can keep main lobes away from the focus and generate Airy-like field with longer nondiffraction length. Considering the cubic phase maps in Fig. 1, this implies that the "eye" part of phase map determines the transverse acceleration of main lobe, but other parts of phase map enlarge the nondiffraction length and produce more minor lobes. Since the modulation index takes a small value, the phase of incident light at the exit aperture is depended on the "eye" part. Then, slow phase modulation inclines the plane wavefront of incident light at certain angle and induces some coma aberration. Thus, the Airy-like field takes on transverse acceleration. On the other hand, since the modulation index takes a relatively large value, the weight of the "eye" part becomes small. This decreases the

effective aperture of incident light with titled wavefront and produces longer nondiffraction length. Meanwhile, fast phase modulation induces interference effect, and generates more minor lobes. In application, modulation index must be selected carefully by the physical parameters of optical system to obtain appropriate Airy-like field.

For the high NA optical system, the tightly focused field is usually affected by the polarization state of incident light [31]. Then, in order to investigate the effect of polarization, the normalized optical fields obtained by different polarized light, such as x-axis linear polarization, circular polarization, radial polarization and azimuthal polarization, are presented in Fig. 4. Here, based on the change trend of Airy-like field shown in Fig. 3, we take $\alpha = 0.004$

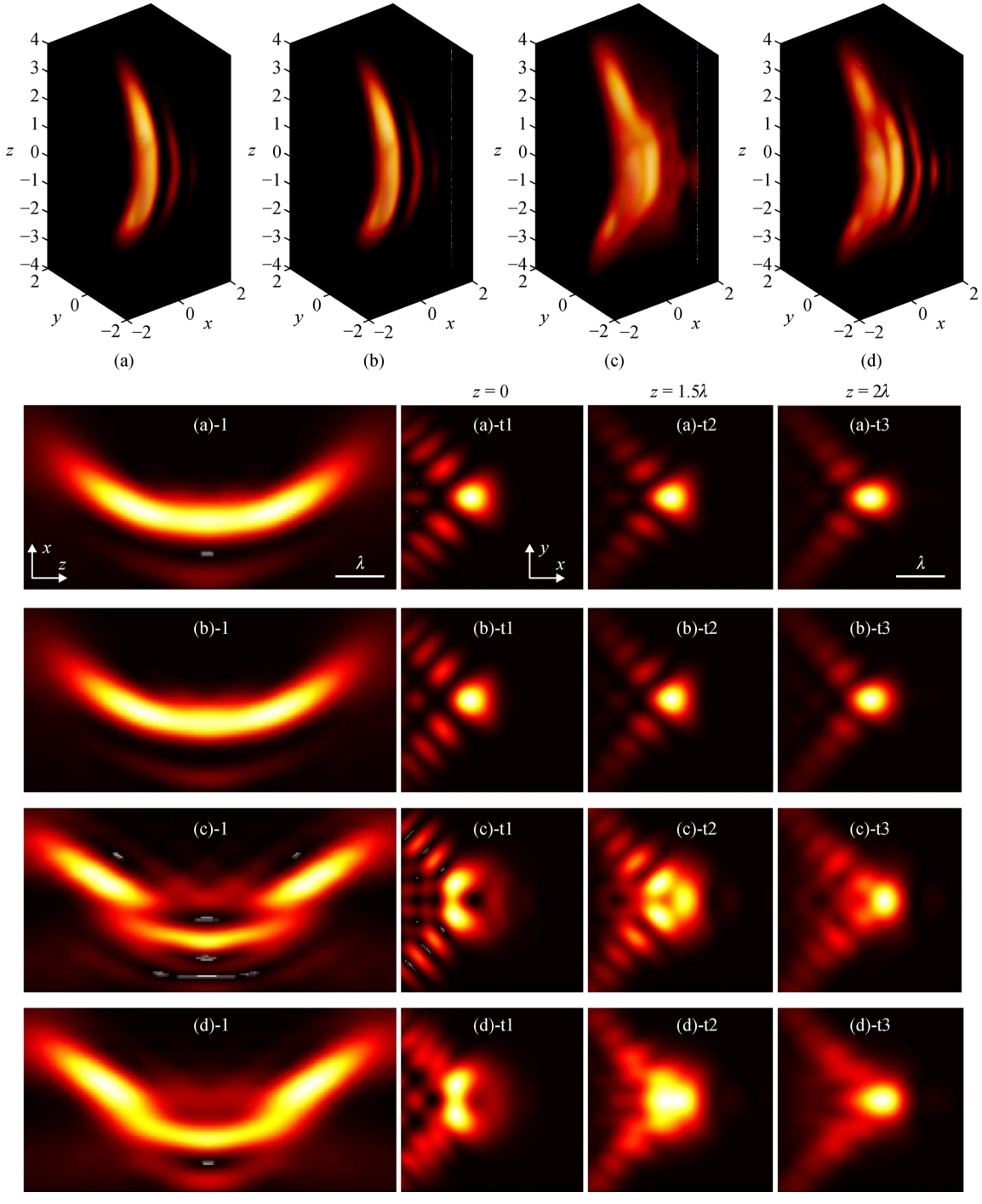

Fig. 4 Normalized optical fields obtained by different polarized lights. The three-dimensional optical fields are (a)–(d) for x-axis linear polarization, circular polarization, azimuthal polarization and radial polarization, respectively. Here, the longitudinal optical fields through the focus are (a)-l–(d)-l, and the transverse optical fields at $z = 0$, 1.5λ and 2λ are (a)-t1–(d)-t3

as an example, and other simulation parameters remain the same. It is noted that, when the polarization state of incident light is spatial uniform, such as linear and circular polarization, Figs. 4(a)-t1 and 4(b)-t1 show that the main lobe of Airy-like field has only one intensity peak and keep clear distance to minor lobes in the focal plane. Along the acceleration trajectory, the Airy-like field depicted in Figs. 4(a)-l and 4(b)-l can hold one main lobe and make the nondiffication length reach approximately 6λ. Furthermore, the Airy-like fields generated by circularly and linearly polarized light have no difference. This is proved by Figs. 4(a) and 4(b). However, when the incident light is azimuthal polarization, Fig. 4(c)-t1 shows the main lobe of Airy-like field has two intensity peaks and also keeps clear distance to minor lobes in the focal plane. In Fig. 4(c)-l, there are two obvious transition areas located from $z = \lambda$ to $z = 2\lambda$, and $z = -2\lambda$ to $z = -\lambda$ along the acceleration trajectory, respectively. Based on Figs. 4(c), 4(c)-l and 4(c)-t, it is found that the transition areas are induced by the change of the main lobe from two-peak mode to one-peak mode, and the change of intensity patterns are discrete. For the case of radially polarized light shown in Figs. 4(d)-l and 4(d)-t, the main lobe also has two intensity peaks in the focal plane and will change into one-peak mode along the acceleration trajectory. However, main lobe cannot keep clear distance to the minor lobe. Compared with Fig. 4(c), it is found that the change of main lobe from two-peak mode to one-peak mode is more successive. Then, for further investigating this difference induced by the azimuthally and radially polarized light, all electric parts of the Airy-like field at $z = 1.5\lambda$ plane, corresponding to Figs. 4(c)-t2 and 4(d)-t2, are shown in Fig. 5. Note that the changes of main lobes are depended on the relative weight of all-electric parts, the electric parts I_x and I_y for radially polarized light are respectively similar to the I_y and I_x for azimuthally polarized light, but a strong longitudinal part I_z is presented for radially polarized light. Thus, transverse parts of the Airy-like field for spatial nonuniform polarization also have similar distribution patterns. This case has been presented for spatial uniform polarization. In addition, the strong longitudinal part I_z can make the Airy-like field take on different change trend for radially polarized light. Therefore, under the high NA optical system, the Airy-like field is affected by spatial nonuniform polarization, and the strong longitudinal part I_z maybe is helpful to produce more complex Airy-like field.

During our simulation, it is also found that the Airy-like field is determined with electric part I_x for the x-axis linearly polarized light. For the circularly polarized light, electric parts I_x and I_y of the Airy-like field have the same distributions, which are similar to the electric part I_x for x-axis linearly polarized light. Justly, this case induces the Airy-like field generated by the circularly polarized light similar to the field for the x-axis linearly polarized light. Based on the relation between linear and circular polarization, the Airy-like field generated by the y-axis linearly polarized light will also be similar to the field for the x-axis linearly polarized light. This phenomenon is different to the general case without cubic phase modulation, where linear polarization often makes the focused field to take on different magnifications along the parallel and perpendicular directions of polarization. So, cubic phase modulation can make the Airy-like field insensitive to the spatial uniform polarization under high NA optical system. However, for the spatial nonuniform polarization such as radial and azimuthal polarization, there are obvious differences in the electric parts I_x, I_y and I_z of the Airy-like field. Compared with the electric part I_x for the x-axis linearly polarized light, these transverse electric parts I_x and I_y have different intensity patterns, but the longitudinal electric part I_z has almost similar intensity pattern. Then, cubic phase modulation mainly affects the transverse parts

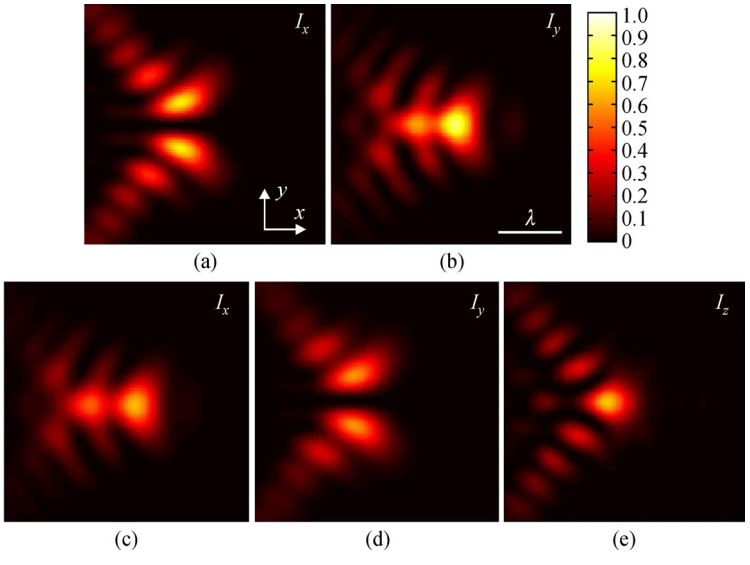

Fig. 5 Electric field parts in the transverse plane at $z = 1.5\lambda$ for (a) and (b) azimuthally and (c)–(e) radially polarized light

of the Airy-like field for the spatial nonuniform polarized light. On the other hand, the intensity of longitudinal part I_z is sensitive to the modulation index. Therefore, for the linearly and circularly polarized light, the Airy-like field generated by cubic phase modulation is mainly depended on the modulation index. However, for the spatial nonuniform polarized light, the Airy-like field is depended on the modulation index and polarization state. In future, the radially polarized light with cubic phase modulation may afford plentiful optical field structures.

4 Conclusion

In this paper, the tightly focused fields of an incident light with cubic phase modulation have been investigated by vectorial diffraction theory. The results show that, when the incident light modulated by cubic phase in the high NA optical system, the Airy-like field with nondiffraction and transverse acceleration will be presented. For the circularly polarized incident light, with the increasing of modulation index in cubic phase, the nondiffraction length of the main lobe will enlarge, but the intensity patterns of the main lobe will transform from uniform to light pearl. Justly due to the change of intensity patterns, there are two transition areas presented at the transverse acceleration trajectory, which is different to the case of Airy beam. In addition, the locations of the main lobe in the focal plane will be far away from the focus. All of these can be attributed to the similar coma aberration and interference effect induced by cubic phase. Meanwhile, cubic phase can make the Airy-like field has different sensitivities to the polarization state of incident light. The Airy-like field for the linearly polarized light is the same as the case of circularly polarized light. However, for the spatial nonuniform polarized light, such as azimuthal and radial polarization, the intensity patterns of the main lobe will transform from two-peak mode to one-peak mode along the acceleration trajectory. This is due to the different distribution of electric parts I_x, I_y and I_z in the Airy-like field. The Airy-like field produced by our method may have great potentials in light manipulation, imaging and surface plasma control.

Acknowledgements This work was supported in part by the National Key Research and Development Program of China (Nos. 2017YFC0110303 and 2016YFF0101400); the National Basic Research Program of China (973 Program) (No. 2015CB352003); the Natural Science Foundation of Zhejiang province (No. LR16F050001); the Fundamental Research Funds for the Central Universities (No. 2017FZA5004); and the Natural Science Foundation of Shanghai (No. 16ZR1412900).

References

1. Berry M V, Balazs N L. Nonspreading wave packets. American Journal of Physics, 1979, 47(3): 264–267
2. Siviloglou G A, Broky J, Dogariu A, Christodoulides D N. Observation of accelerating Airy beams. Physical Review Letters, 2007, 99(21): 213901
3. Jia S, Vaughan J C, Zhuang X. Isotropic three-dimensional super-resolution imaging with a self-bending point spread function. Nature Photonics, 2014, 8(4): 302–306
4. Vettenburg T, Dalgarno H I C, Nylk J, Coll-Lladó C, Ferrier D E K, Čižmár T, Gunn-Moore F J, Dholakia K. Light-sheet microscopy using an Airy beam. Nature Methods, 2014, 11(5): 541–544
5. Chong A, Renninger W H, Christodoulides D N, Wise F W. Airy-Bessel wave packets as versatile linear light bullets. Nature Photonics, 2010, 4(2): 103–106
6. Abdollahpour D, Suntsov S, Papazoglou D G, Tzortzakis S. Spatiotemporal airy light bullets in the linear and nonlinear regimes. Physical Review Letters, 2010, 105(25): 253901
7. Baumgartl J, Mazilu M, Dholakia K. Optically mediated particle clearing using Airy wavepackets. Nature Photonics, 2008, 2(11): 675–678
8. Zhang P, Prakash J, Zhang Z, Mills M S, Efremidis N K, Christodoulides D N, Chen Z. Trapping and guiding microparticles with morphing autofocusing Airy beams. Optics Letters, 2011, 36 (15): 2883–2885
9. Liu W, Neshev D N, Shadrivov I V, Miroshnichenko A E, Kivshar Y S. Plasmonic Airy beam manipulation in linear optical potentials. Optics Letters, 2011, 36(7): 1164–1166
10. Belafhal A, Ez-Zariy L, Hennani S, Nebdi H. Theoretical introduction and generation method of a novel nondiffracting waves: Olver beams. Optics and Photonics Journal, 2015, 5(7): 234–246
11. Khonina S N, Ustinov A V. Fractional Airy beams. Journal of the Optical Society of America A, Optics, Image Science, and Vision, 2017, 34(11): 1991–1999
12. Efremidis N K, Christodoulides D N. Abruptly autofocusing waves. Optics Letters, 2010, 35(23): 4045–4047
13. Khonina S N, Porfirev A P, Ustinov A V. Sudden autofocusing of superlinear chirp beams. Journal of Optics, 2018, 20(2): 025605
14. Siviloglou G A, Christodoulides D N. Accelerating finite energy Airy beams. Optics Letters, 2007, 32(8): 979–981
15. Ellenbogen T, Voloch-Bloch N, Ganany-Padowicz A, Arie A. Nonlinear generation and manipulation of Airy beams. Nature Photonics, 2009, 3(7): 395–398
16. Dolev I, Ellenbogen T, Voloch-Bloch N, Arie A. Control of free space propagation of Airy beams generated by quadratic nonlinear photonic crystals. Applied Physics Letters, 2009, 95(20): 201112
17. Dai H T, Sun X W, Luo D, Liu Y J. Airy beams generated by a binary phase element made of polymer-dispersed liquid crystals. Optics Express, 2009, 17(22): 19365–19370
18. Luo D, Dai H T, Sun X W, Demir H V. Electrically switchable finite energy Airy beams generated by a liquid crystal cell with patterned electrode. Optics Communications, 2010, 283(20): 3846–3849
19. Gecevicius M, Beresna M, Kazansky P G. Accelerating Airy beams generated by ultrafast laser induced space- variant nanostructures in glass. In: Proceedings of 2012 Conference on Lasers and Electro-Optics (CLEO). San Jose, CA: IEEE, 2012
20. Cao R, Yang Y, Wang J G, Bu J, Wang M W, Yuan X C. Microfabricated continuous cubic phase plate induced Airy beams for optical manipulation with high power efficiency. Applied

Physics Letters, 2011, 99(26): 261106
21. Cottrell D M, Davis J A, Hazard T M. Direct generation of accelerating Airy beams using a 3/2 phase-only pattern. Optics Letters, 2009, 34(17): 2634–2636
22. Froehly L, Courvoisier F, Mathis A, Jacquot M, Furfaro L, Giust R, Lacourt P A, Dudley J M. Arbitrary accelerating micron-scale caustic beams in two and three dimensions. Optics Express, 2011, 19(17): 16455–16465
23. Singh B K, Remez R, Tsur Y, Arie A. Super-Airy beam: self-accelerating beam with intensified main lobe. Optics Letters, 2015, 40(20): 4703–4706
24. Torre A. Airy beams beyond the paraxial approximation. Optics Communications, 2010, 283(21): 4146–4165
25. Carretero L, Acebal P, Blaya S, García C, Fimia A, Madrigal R, Murciano A. Nonparaxial diffraction analysis of Airy and SAiry beams. Optics Express, 2009, 17(25): 22432–22441
26. Bar-David J, Voloch-Bloch N, Mazurski N, Levy U. Unveiling the propagation dynamics of self-accelerating vector beams. Scientific Reports, 2016, 6(1): 34272
27. Weng X, Song Q, Li X, Gao X, Guo H, Qu J, Zhuang S. Free-space creation of ultralong anti-diffracting beam with multiple energy oscillations adjusted using optical pen. Nature Communications, 2018, 9(1): 5035
28. Cohen N, Yang S, Andalman A, Broxton M, Grosenick L, Deisseroth K, Horowitz M, Levoy M. Enhancing the performance of the light field microscope using wavefront coding. Optics Express, 2014, 22(20): 24817–24839
29. King S V, Doblas A, Patwary N, Saavedra G, Martínez-Corral M, Preza C. Spatial light modulator phase mask implementation of wavefront encoded 3D computational-optical microscopy. Applied Optics, 2015, 54(29): 8587–8595
30. Richards B, Wolf E. Electromagnetic diffraction in optical systems. 2. Structure of the image field in an aplanatic system. Proceedings of the Royal Society of London. Series A, Mathematical and Physical Sciences, 1959, 253(1274): 358–379
31. Hao X, Kuang C F, Wang T T, Liu X. Effects of polarization on the de-excitation dark focal spot in STED microscopy. Journal of Optics, 2010, 12(11): 115707

Yong Liu obtained his Ph.D. degree from University of Shanghai for Science and Technology, Shanghai, China, in 2007. Currently, he is an associate professor at Shanghai University of Electric Power, Shanghai, China. His research interests are point spread function engineering and new imaging method. He focuses on optical microscopy imaging and optical coherence tomography.

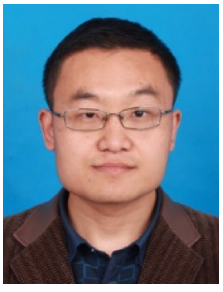

Zhifeng Zhang received his Ph.D. degree in optical engineering from Beijing Jiaotong University. He is an associate professor and a Master tutor at the Zhengzhou University of Light Industry. His research interests are mainly in research and design of novel optical instruments and computer imaging technique.

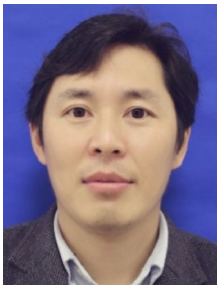

Cuifang Kuang obtained his Ph.D. degree from Beijing Jiaotong University, Beijing, China, in 2007. Currently, he is a professor at Zhejiang University, Hangzhou, China. He recently focuses on optical superresolution and optical microscopy imaging.